International Journal of Thermophysics, Vol. 28, No. 5, October 2007 (© 2007)
DOI: 10.1007/s10765-007-0212-0

Thermophysical Properties of U–Mo/Al Alloy Dispersion Fuel Meats[1]

S. H. Lee,[2,3] J. M. Park,[4] and C. K. Kim[4]

Uranium–molybdenum alloy dispersion fuel meats are being studied for utilization as a research reactor fuel. Thermophysical properties of U–Mo/Al dispersion fuel, where U–Mo was dispersed in aluminum in research reactor fuel for the study, were determined by computing the thermal conductivity through measurements of the specific heat capacity and thermal diffusivity. Uranium molybdenum powder was first fabricated and utilized as U–Mo/Al dispersion fuel; the molybdenum-to-uranium ratios were 6, 8, and 10 mass% to produce the initial powder, which was then combined with aluminum (Al 1060). The volume fractions of U–Mo powder to aluminum were 10, 30, 40, and 50 vol.% to fabricate the dispersion fuel. The thermal diffusivity and specific heat capacity were measured by the laser-flash and differential scanning calorimetry (DSC) methods, respectively. Although the thermal diffusivity showed a decreasing trend with the U–Mo volume fraction when the dispersion quantity was insignificant, the trend reversed with a higher dispersion level. The specific heat capacity increases monotonically with temperature; its value is larger for a smaller dispersion level. Additionally, the overall thermal conductivity increases with temperature. Finally, the thermal conductivity decreases with an increase in the amount of U–Mo powder in the dispersion fuel.

KEY WORDS: dispersion fuel; specific heat capacity; thermal conductivity; thermal diffusivity; uranium–molybdenum alloy.

[1]Paper presented at the Seventeenth European Conference on Thermophysical Properties, September 5–8, 2005, Bratislava, Slovak Republic.

[2]Division of Physical Metrology, Korea Research Institute of Standards and Science, 1 Doryong-dong, Yuseong-gu, Daejeon 305-340, Korea.
[3]To whom correspondence should be addressed. E-mail: leesh@kriss.re.kr
[4]Korea Atomic Energy Research Institute, 150 Dukjin-dong, Yuseong-gu, Daejeon 306-353, Korea.

1. INTRODUCTION

In order to reduce the uranium enrichment of a research and test reactor fuel, dispersion fuels such as uranium–molybdenum fuel particles dispersed in an aluminum base material are being developed [1–3]. The Reduced Enrichment for Research and Test Reactors (RERTR) program is developing stable fuel in fabrication and irradiation of dispersion type with high-uranium density for nuclear non-proliferation. There are reports of fuel development using U–Si, U–Zr, U–Mo, and U–Nb among various materials [4]; furthermore, the U–Mo alloy is the most promising candidate for materials in the research and test reactor fuel. Several Time–Temperature–Transformation (TTT) curves for U–8 mass% Mo and U–10 mass% Mo predict minimal transformation of the cubic γ phase during fabrication [5]. The U–Mo dispersion fuel, which has been developed for a high performance research reactor fuel with a very high uranium density, was found to be reprocessable. The fabrication process and irradiation behavior of atomized U–Mo alloy dispersion fuel has been reported [6, 7].

In the application of a research and test reactor fuel, the thermophysical properties are key parameters to ascertain the core temperature of the fuel and to optimize the thermal design. In this study, we provide results for the thermal conductivity, thermal diffusivity, and the specific heat capacity as basic data in thermal design. Here, the thermal diffusivity was measured by the laser-flash method using fabricated U–Mo/Al dispersion fuel and the specific heat capacity was measured using a differential scanning calorimeter (DSC). The thermal conductivity was calculated from the measured thermal diffusivity and specific heat capacity. For the dispersion material, uranium–molybdenum was used; the quantity of molybdenum to uranium was 6, 8, and 10 mass% for powder fabrication and the base material was aluminum (Al 1060). The dispersion fuel meats were prepared by adding 10, 30, 40, and 50 vol.% of U–Mo powder with aluminum. Two types of uranium–molybdenum dispersion materials fabricated by a centrifugal atomized method and a conventional comminution method were used.

2. EXPERIMENTAL

2.1. Sample Preparation

Samples for the thermal diffusivity and specific heat capacity measurements are described in Table I. For U–Mo powder fabrication, concentrations of molybdenum relative to uranium of 6, 8, and 10 mass% were added to produce the powder. The U–Mo fuel powder was fabricated by

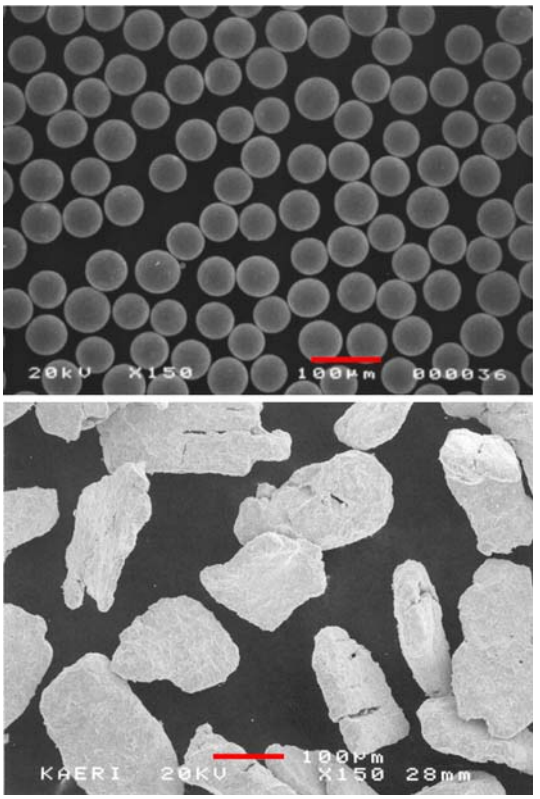

Fig. 1. SEM photo of U–Mo particles fabricated by atomized and comminution methods.

using a centrifugal atomized method and a comminution method [6,7]. Figure 1 shows a photograph of the U–Mo fuel powder fabricated by using these methods. The mean diameters of U–Mo particles fabricated by the centrifugal atomized method were approximately 50–70 μm and by the comminution method were approximately 80–90 μm. Compared to the regular and round shapes of powders fabricated by the centrifugal atomized method, the comminuted powders were extremely irregular.

Samples for thermophysical property measurements were fabricated by combining U–Mo powder and aluminum. The dispersion quantity of U–Mo powder, fabricated by the atomized method, was fixed at 10, 30, 40, and 50 vol.% in aluminum for four different samples. On the other hand, the dispersion fuel fabricated by the comminution method was fixed at 10 mass% of molybdenum and the U–10 mass% Mo volume fractions were fixed at 10, 30, and 50 vol.% in aluminum for three different

Table I. Samples of U–Mo/Al Dispersion Fuel Meats

Sample ID	Sample description	U–Mo (vol.% in meat)	Density ($g \cdot cm^{-3}$)			Thermal conductivity[c] ($W \cdot m^{-1} K^{-1}$)
			DSC[a]	LF[b]	Theoretical	
U10M_A10	U–10 mass% Mo/Al atomized method	10	3.69	4.12	4.13	197.2
U10M_A30		30	7.08	7.00	7.00	128.7
U10M_A40		40	8.71	8.69	8.43	96.5
U10M_A50		50	9.85	9.80	9.86	73.0
U8M_A10	U–8 mass% Mo/Al atomized method	10	4.16	4.16	4.17	180.3
U8M_A30		30	7.27	7.15	7.10	124.2
U8M_A40		40	9.36	9.20	8.56	93.9
U8M_A50		50	10.81	10.54	10.03	66.8
U6M_A10	U–6 mass% Mo/Al atomized method	10	4.23	4.19	4.20	183.1
U6M_A30		30	7.30	7.22	7.20	131.3
U6M_A40		40	8.68	8.76	8.70	107.5
U6M_A50		50	10.20	10.26	10.21	82.5
U10M_P10	U–10 mass% Mo/Al comminution method	10	4.16	4.08	4.13	180.8
U10M_P30		30	7.20	7.00	7.00	119.3
U10M_P50		50	8.61	8.05	9.86	38.3

[a] DSC: samples for specific heat capacity measurements.
[b] LF: samples for thermal diffusivity measurements.
[c] Room temperature values.

samples. Fifteen different samples were fabricated by the centrifugal atomized method and the comminution method into three sets for each of the thermal conductivity and specific heat capacity measurements, giving a total of 90 samples for the study.

2.2. Thermophysical Property Measurements [1,8]

For thermal diffusivity measurements a laser-flash method (Sinku-Riko, TC-7000VH/L) was used for measurements at temperatures up to 500°C. The thermal diffusivity was analyzed using the Parker method [9]. The results were calculated using the half time of the maximum temperature increase on the back of the sample for the thermal diffusivity. The temperature measurement on the back of the sample was conducted using an InSb infrared sensor. Moreover, the temperature was controlled by using a tungsten mesh heater in vacuum. For consistent heating energy on the sample, the front and back of the sample were sprayed with graphite. The sample for laser-flash measurements was a disk of about 2 mm in thickness and about 7 mm in diameter. Thermal diffusivity data were corrected by Azumi and Takahashi's method [10] to decrease the effect of a finite pulse. The mean value was computed from five measurements of the thermal diffusivity. Furthermore, the standard deviation and reproducibility of the thermal diffusivity measurements was estimated to be approximately 3% based on measurements on poco-graphite (NIST SRM 8245) from room temperature to 1300°C.

The specific heat capacity was measured with a DSC (Perkin–Elmer Pyris 1) at temperatures up to 380°C at 20°C intervals. Moreover, it was measured at a temperature increase rate of $5\,\mathrm{K}\cdot\mathrm{min}^{-1}$ and a flow rate of nitrogen at $30\,\mathrm{mL}\cdot\mathrm{min}^{-1}$. Synthetic sapphire, NIST SRM 720, was used as a specific heat capacity comparative standard reference material; the standard deviation and reproducibility of the specific heat capacity measurements was estimated to be approximately 2% based on measurements from room temperature to 500°C on the synthetic sapphire SRM.

The thermal conductivity $\lambda(\mathrm{W}\cdot\mathrm{m}^{-1}\cdot\mathrm{K}^{-1})$ was computed using

$$\lambda = \rho\alpha C_p \tag{1}$$

where ρ is the density $(\mathrm{g}\cdot\mathrm{cm}^{-3})$, α is the thermal diffusivity $(\mathrm{cm}^2\cdot\mathrm{s}^{-1})$, and C_p is the specific heat capacity $(\mathrm{J}\cdot\mathrm{g}^{-1}\cdot\mathrm{K}^{-1})$.

3. RESULTS AND DISCUSSION

The density differences in the samples used for measuring the dispersion fuel's thermal diffusivity and specific heat capacity were approximately

Table II. Experimental Results for the Thermal Diffusivity of U–10 mass% Mo/Al Dispersion Fuel Fabricated by Atomized Method

Sample T (°C)	U10M_A10 ($cm^2 \cdot s^{-1}$)	U10M_A30 ($cm^2 \cdot s^{-1}$)	U10M_A40 ($cm^2 \cdot s^{-1}$)	U10M_A50 ($cm^2 \cdot s^{-1}$)
25	0.7804	0.5452	0.4141	0.3139
100	0.7764	0.5394	0.4259	0.3236
200	0.7549	0.5391	0.4180	0.3130
300	0.7377	0.5370	0.4232	0.3442
400	0.7104	0.5212	0.4234	0.3519
500	0.6722	0.5018	0.4124	0.3469

within 3% except for the 10 Vol.% sample, and the distributions were even. For the thermal diffusivity and specific heat capacity measurements, three specimens were fabricated for each measurement and the thermal conductivity was computed from the average values of measurements on these three specimens. According to the literature, the densities of aluminum, uranium, and molybdenum at 293 K are 2.698, 18.950, and 10.220 $g \cdot cm^{-3}$ [11], respectively. Since there is a large difference between aluminum and uranium densities, the differences in density for different volume fractions of U–Mo were also large, and this had a significant effect on the thermal conductivity. The density of U–Mo/Al dispersion fuels varied from approximately 3.6 to 10.8 $g \cdot cm^{-3}$, according to the volume fraction of U–Mo particles.

The thermal diffusivity of dispersion fuels was measured in the temperature range from 25 to 500°C as shown in Table II–V. The thermal diffusivity decreased with an increase in temperature when the U–Mo volume fraction was small. However, as the U–Mo volume fraction increased, the thermal diffusivity also increased with temperature. The thermal diffusivity differences using the comminution method were found to be within 1.5% of one another when the U–Mo volume fraction was 10 vol.%.

Although the effects of U–Mo appeared to be insignificant when the volume fraction was small, with larger volume fractions, the thermal resistance for irregular U–Mo particles increased such that the comminution method gave a smaller thermal diffusivity than that from the centrifugal atomized method. A third-order polynomial was fitted to the thermal diffusivity data to calculate the thermal conductivity.

The specific heat capacity was measured at temperatures from 25 to 380°C as shown in Table VI–IX. The specific heat capacity for all specimens increased monotonically with temperature. For example, the specific heat capacities of U–10 mass% Mo/Al at 26.1°C were 0.6455,

Table III. Experimental Results for the Thermal Diffusivity of U–8 mass% Mo/Al Dispersion Fuel Fabricated by Atomized Method

Sample T (°C)	U8M_A10 ($cm^2 \cdot s^{-1}$)	U8M_A30 ($cm^2 \cdot s^{-1}$)	U8M_A40 ($cm^2 \cdot s^{-1}$)	U8M_A50 ($cm^2 \cdot s^{-1}$)
25	0.7773	0.5401	0.4026	0.2967
100	0.7704	0.5510	0.4109	0.3042
200	0.7428	0.5414	0.4083	0.3121
300	0.7276	0.5304	0.4055	0.3128
400	0.7010	0.5160	0.4077	0.3167
500	0.6725	0.4987	0.4009	0.3123

Table IV. Experimental Results for the Thermal Diffusivity of U–6 mass% Mo/Al Dispersion Fuel Fabricated by Atomized Method

Sample T (°C)	U6M_A10 ($cm^2 \cdot s^{-1}$)	U6M_A30 ($cm^2 \cdot s^{-1}$)	U6M_A40 ($cm^2 \cdot s^{-1}$)	U6M_A50 ($cm^2 \cdot s^{-1}$)
25	0.7864	0.5506	0.4544	0.3463
100	0.7824	0.5696	0.4705	0.3491
200	0.7620	0.5624	0.4610	0.3478
300	0.7336	0.5450	0.4600	0.3533
400	0.7036	0.5305	0.4529	0.3566
500	0.6679	0.5123	0.4435	0.3537

0.3356, 0.2663, and $0.2342\,J \cdot g^{-1} \cdot K^{-1}$ depending on the volume fraction. These substantial differences are correlated with the amount of uranium. The reference values of specific heat capacity are 0.9025, 0.1162, and $0.2508\,J \cdot g^{-1} \cdot K^{-1}$ for aluminum, uranium, and molybdenum, respec-

Table V. Experimental Results for the Thermal Diffusivity of U–10 mass% Mo/Al Dispersion Fuel Fabricated by Comminution Method

Sample T (°C)	U10M_P10 ($cm^2 \cdot s^{-1}$)	U10M_P30 ($cm^2 \cdot s^{-1}$)	U10M_P50 ($cm^2 \cdot s^{-1}$)
25	0.7921	0.5139	0.1917
100	0.7678	0.5110	0.1916
200	0.7463	0.4947	0.1904
300	0.7444	0.4981	0.2054
400	0.7209	0.4897	0.2121
500	0.6784	0.4673	0.2130

Table VI. Specific Heat Capacity of U–10 mass% Mo/Al Dispersion Fuel Fabricated by Atomized Method

Sample T (°C)	U10M_A10 ($J \cdot g^{-1} \cdot K^{-1}$)	U10M_A30 ($J \cdot g^{-1} \cdot K^{-1}$)	U10M_A40 ($J \cdot g^{-1} \cdot K^{-1}$)	U10M_A50 ($J \cdot g^{-1} \cdot K^{-1}$)
26.1	0.6455	0.3356	0.2663	0.2342
41.1	0.6553	0.3403	0.2699	0.2372
61.2	0.6653	0.3451	0.2737	0.2402
81.3	0.6746	0.3496	0.2770	0.2431
101.3	0.6828	0.3535	0.2800	0.2456
121.3	0.6898	0.3568	0.2826	0.2478
141.3	0.6971	0.3604	0.2853	0.2500
161.2	0.7039	0.3639	0.2879	0.2522
181.3	0.7101	0.3672	0.2905	0.2544
201.2	0.7173	0.3701	0.2926	0.2561
221.2	0.7233	0.3729	0.2950	0.2582
241.2	0.7283	0.3759	0.2973	0.2602
261.1	0.7350	0.3788	0.2996	0.2622
281.2	0.7388	0.3812	0.3015	0.2638
301.2	0.7440	0.3842	0.3037	0.2652
321.2	0.7487	0.3865	0.3065	0.2677
341.3	0.7542	0.3891	0.3090	0.2698
361.2	0.7588	0.3928	0.3124	0.2723
381.2	0.7631	0.3962	0.3151	0.2758

tively. The specific heat capacity of aluminum is comparatively much larger than that for uranium; thus, the sample with a smaller amount of U–Mo dispersion and a larger aluminum content has a higher specific heat capacity. The specific heat capacity data were fitted with a third-order polynomial for calculating thermal conductivities.

The thermal conductivity of U–Mo/Al dispersion fuels at temperatures from 25 to 380°C obtained from the measured thermal diffusivity, specific heat capacity, and density data are shown in Tables X–XIII and Figs. 2–4. The thermal conductivity of the dispersion fuels decreased as the volume fraction of U–Mo particles increased. Figure 2 indicates that the dispersion fuels fabricated by the centrifugal atomized method have a higher thermal conductivity than those fabricated by the comminution method. The differences in the thermal conductivity were larger when the U–Mo volume fraction was larger than 50 vol.%. When the volume fraction was 10 vol.%, the difference was within approximately 1.5% of the measurement uncertainty range; the thermal conductivity of the comminution method specimen was lower than that for the centrifugal atomized

Table VII. Specific Heat Capacity of U–8 mass% Mo/Al Dispersion Fuel Fabricated by Atomized Method

Sample T (°C)	U8M_A10 ($J \cdot g^{-1} \cdot K^{-1}$)	U8M_A30 ($J \cdot g^{-1} \cdot K^{-1}$)	U8M_A40 ($J \cdot g^{-1} \cdot K^{-1}$)	U8M_A50 ($J \cdot g^{-1} \cdot K^{-1}$)
26.1	0.5570	0.3169	0.2494	0.2113
41.1	0.5653	0.3219	0.2533	0.2114
61.2	0.5742	0.3263	0.2572	0.2174
81.3	0.5820	0.3306	0.2602	0.2200
101.3	0.5893	0.3343	0.2635	0.2225
121.3	0.5952	0.3378	0.2667	0.2250
141.3	0.6009	0.3408	0.2694	0.2273
161.2	0.6066	0.3442	0.2721	0.2293
181.3	0.6124	0.3469	0.2745	0.2313
201.2	0.6176	0.3503	0.2774	0.2338
221.2	0.6231	0.3527	0.2799	0.2359
241.2	0.6281	0.3558	0.2828	0.2379
261.1	0.6330	0.3589	0.2852	0.2401
281.2	0.6353	0.3641	0.2885	0.2430
301.2	0.6409	0.3668	0.2920	0.2460
321.2	0.6440	0.3645	0.2938	0.2475
341.3	0.6496	0.3689	0.2960	0.2492
361.2	0.6606	0.3682	0.2969	0.2505
381.2	0.6692	0.3693	0.2970	0.2535

method specimen by approximately 6–8% at 30 vol.%. Furthermore, for a 50 vol.% sample, the difference was substantial at approximately 40%.

Although the effect of the thermal conductivity of aluminum is substantial when the volume fraction was small, as the volume fraction increased, the irregularity of the U–Mo particle specimen using the comminution method showed a larger effect on the thermal conductivity resistance than the specimens using the centrifugal atomized method that were fabricated into regular-shaped particles. Generally, the thermal conductivity increased with an increase in temperature; however, it was somewhat diminished near 300°C for some of the specimens. Nevertheless, this was considered to be well within the uncertainty of the measurements. On the other hand, it was estimated that U6M's 10 and 30 vol.% specimens showed a decreasing trend near 300°C.

Figures 5 to 7 show plots of the thermal conductivity for different U–Mo volume fractions of the dispersion fuel. The thermal conductivity of the dispersion fuels depends on the quantity of U–Mo; it decreases significantly as the volume fraction increases. The density of uranium had a significant effect on the thermal conductivity of the dispersion fuels.

Table VIII. Specific Heat Capacity of U–6 mass% Mo/Al Dispersion Fuel Fabricated by Atomized Method

Sample T (°C)	U6M_A10 ($J \cdot g^{-1} \cdot K^{-1}$)	U6M_A30 ($J \cdot g^{-1} \cdot K^{-1}$)	U6M_A40 ($J \cdot g^{-1} \cdot K^{-1}$)	U6M_A50 ($J \cdot g^{-1} \cdot K^{-1}$)
26.1	0.5507	0.3256	0.2678	0.2304
41.1	0.5615	0.3307	0.2728	0.2338
61.2	0.5711	0.3360	0.2773	0.2375
81.3	0.5793	0.3405	0.2810	0.2406
101.3	0.5869	0.3447	0.2835	0.2434
121.3	0.5949	0.3488	0.2879	0.2460
141.3	0.6012	0.3527	0.2906	0.2485
161.2	0.6083	0.3562	0.2933	0.2507
181.3	0.6146	0.3598	0.2965	0.2533
201.2	0.6217	0.3639	0.2998	0.2556
221.2	0.6280	0.3676	0.3030	0.2582
241.2	0.6325	0.3712	0.3065	0.2609
261.1	0.6392	0.3762	0.3104	0.2644
281.2	0.6447	0.3812	0.3150	0.2689
301.2	0.6513	0.3867	0.3203	0.2736
321.2	0.6537	0.3874	0.3229	0.2749
341.3	0.6570	0.3888	0.3223	0.2771
361.2	0.6572	0.3868	0.3226	0.2754
381.2	0.6639	0.3892	0.3251	0.2749

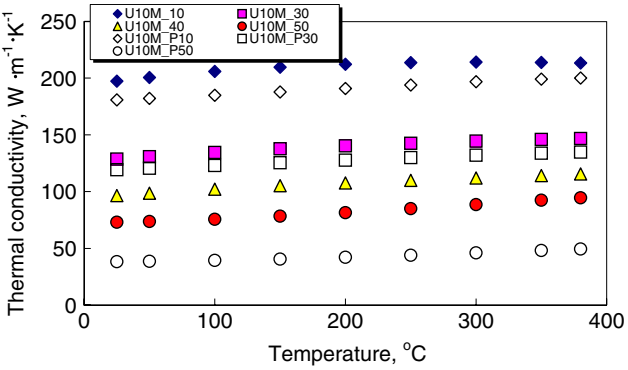

Fig. 2. Thermal conductivity of U–10 mass% Mo/Al fabricated by atomized and comminution methods.

Table IX. Specific Heat Capacity of U–10 mass% Mo/Al Dispersion Fuel Fabricated by Comminution Method

Sample T (°C)	U10M_P10 ($J \cdot g^{-1} \cdot K^{-1}$)	U10M_P30 ($J \cdot g^{-1} \cdot K^{-1}$)	U10M_P50 ($J \cdot g^{-1} \cdot K^{-1}$)
26.1	0.5527	0.3254	0.2388
41.1	0.5621	0.3299	0.2416
61.2	0.5712	0.3346	0.2449
81.3	0.5794	0.3391	0.2478
101.3	0.5873	0.3434	0.2508
121.3	0.5934	0.3464	0.2529
141.3	0.6006	0.3502	0.2554
161.2	0.6066	0.3535	0.2574
181.3	0.6117	0.3566	0.2598
201.2	0.6193	0.3606	0.2622
221.2	0.6208	0.3613	0.2608
241.2	0.6300	0.3662	0.2656
261.1	0.6350	0.3688	0.2677
281.2	0.6357	0.3693	0.2682
301.2	0.6479	0.3760	0.2727
321.2	0.6544	0.3790	0.2753
341.3	0.6560	0.3809	0.2768
361.2	0.6583	0.3811	0.2775
381.2	0.6681	0.3874	0.2817

Table X. Thermal Conductivity of U–10 mass% Mo/Al Dispersion Fuel Fabricated by Atomized Method

Sample T (°C)	U10M_A10 ($W \cdot m^{-1} \cdot K^{-1}$)	U10M_A30 ($W \cdot m^{-1} \cdot K^{-1}$)	U10M_A40 ($W \cdot m^{-1} \cdot K^{-1}$)	U10M_A50 ($W \cdot m^{-1} \cdot K^{-1}$)
25	197.2	128.7	96.5	73.0
50	200.5	130.8	98.6	73.7
100	205.8	134.5	102.2	75.7
150	209.7	137.7	105.2	78.3
200	212.2	140.3	107.7	81.4
250	213.7	142.6	109.9	84.9
300	214.1	144.4	112.0	88.6
350	213.8	146.0	114.1	92.4
380	213.3	146.7	115.5	94.6

Table XI. Thermal Conductivity of U–8 mass% Mo/Al Dispersion Fuel Fabricated by Atomized Method

Sample T (°C)	U8M_A10 ($W \cdot m^{-1} \cdot K^{-1}$)	U8M_A30 ($W \cdot m^{-1} \cdot K^{-1}$)	U8M_A40 ($W \cdot m^{-1} \cdot K^{-1}$)	U8M_A50 ($W \cdot m^{-1} \cdot K^{-1}$)
25	180.3	124.2	93.9	66.8
50	183.4	127.0	95.8	68.6
100	187.8	131.6	99.5	72.1
150	190.4	135.1	102.7	75.1
200	191.8	137.6	105.6	77.7
250	192.6	139.0	108.0	80.1
300	193.4	139.3	110.0	82.2
350	194.6	138.8	111.5	84.2
380	195.9	138.1	112.3	85.3

Table XII. Thermal Conductivity of U–6 mass% Mo/Al Dispersion Fuel Fabricated by Atomized Method

Sample T (°C)	U6M_A10 ($W \cdot m^{-1} \cdot K^{-1}$)	U6M_A30 ($W \cdot m^{-1} \cdot K^{-1}$)	U6M_A40 ($W \cdot m^{-1} \cdot K^{-1}$)	U6M_A50 ($W \cdot m^{-1} \cdot K^{-1}$)
25	183.1	131.3	107.5	82.5
50	186.8	134.8	110.0	83.4
100	192.7	141.0	114.6	85.8
150	196.9	145.9	118.8	88.7
200	199.6	149.5	122.3	91.9
250	200.8	151.6	125.1	95.0
300	200.6	152.2	127.1	97.8
350	199.2	151.5	128.3	100.0
380	197.9	150.4	128.6	100.8

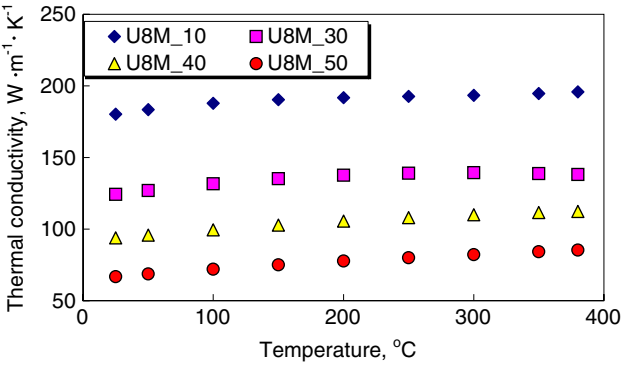

Fig. 3. Thermal conductivity of U–8 mass% Mo/Al fabricated by atomized method.

Table XIII. Thermal Conductivity of U–10 mass% Mo/Al Dispersion Fuel Fabricated by Comminution Method

Sample T (°C)	U10M_P10 ($W \cdot m^{-1} \cdot K^{-1}$)	U10M_P30 ($W \cdot m^{-1} \cdot K^{-1}$)	U10M_P50 ($W \cdot m^{-1} \cdot K^{-1}$)
25	180.8	119.3	38.3
50	182.1	120.5	38.6
100	184.9	123.0	39.4
150	187.8	125.4	40.6
200	190.9	127.7	42.2
250	194.0	129.9	44.0
300	196.8	132.0	46.0
350	199.1	133.8	48.2
380	200.1	134.7	49.5

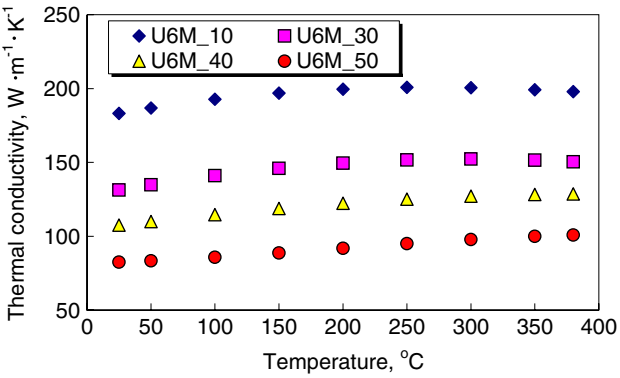

Fig. 4. Thermal conductivity of U–6 mass% Mo/Al fabricated by atomized method.

Literature values of the thermal conductivity of aluminum, uranium, and molybdenum are 237, 27.6, and 138 $W \cdot m^{-1} \cdot K^{-1}$ [11], respectively. In comparison to the basic material, aluminum, the thermal conductivity of uranium is substantially less; thus, the amount of uranium had a predominant impact on the thermal conductivity.

Figure 8 shows comparisons of the thermal conductivity in materials containing similar quantities of uranium as the U–Mo/Al dispersion fuels in this study. The density of ANL samples TP2 and TP3 [12] were 10.06 and 8.29 $g \cdot cm^{-3}$, respectively; the uranium loading densities were approximately 6 and 8 $gU \cdot cm^{-3}$, respectively. The U10Mo_A40 and U10M_A50 specimens used in this study had densities of 8.69 and 9.89 $g \cdot cm^{-3}$, respectively. The uranium loading densities were 6.1 and 7.7 $gU \cdot cm^{-3}$,

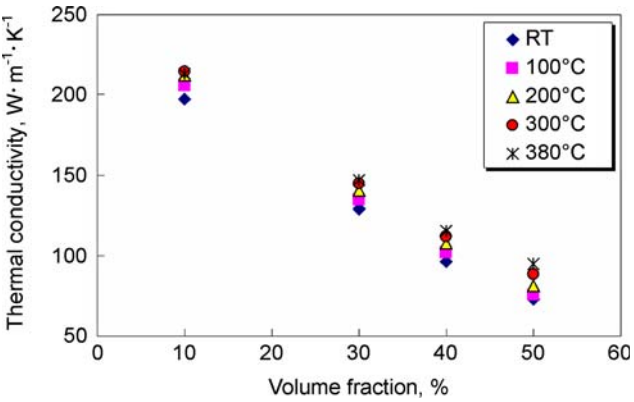

Fig. 5. Thermal conductivity of U–10 mass% Mo/Al per U–10 mass% Mo volume fraction fabricated by atomized method.

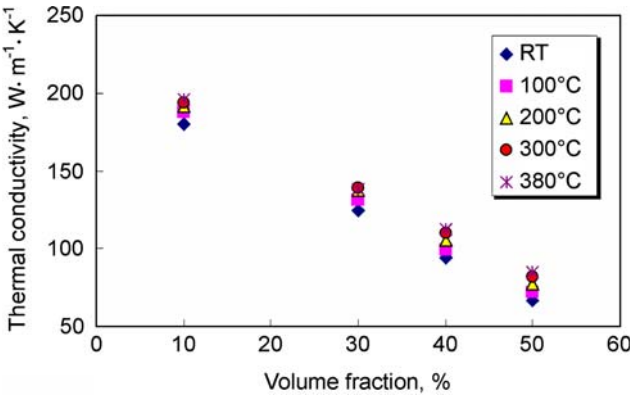

Fig. 6. Thermal conductivity of U–8 mass% Mo/Al pursuant to U–8 mass% Mo volume fraction fabricated by atomized method.

respectively, which were closest to the ANL sample in uranium content. The results of this study revealed that there was a trend of the thermal conductivity increasing monotonically with temperature. In particular, other than for some of the TP3-6 and TP3-7 results, the overall data matched within about 5% (Table XIV).

Figure 9 shows the thermal conductivity of all specimens used in dispersion fuels at different temperatures and uranium loading densities. The uranium loading density of the samples used in this study ranged from 1.5 to 8.5 $gU \cdot cm^{-3}$. The thermal conductivity decreased monotonically as

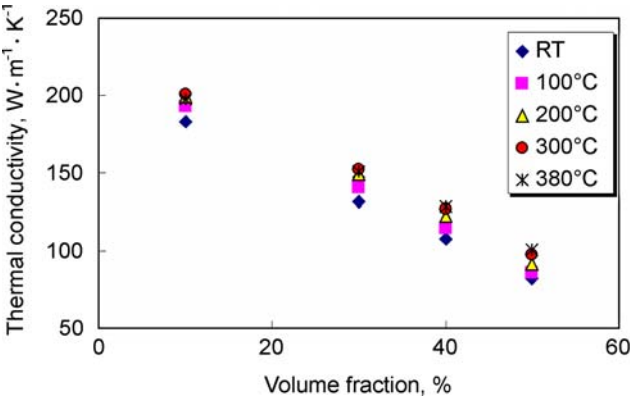

Fig. 7. Thermal conductivity of U–6 mass% Mo/Al per U–6 mass% Mo volume fraction fabricated by atomized method.

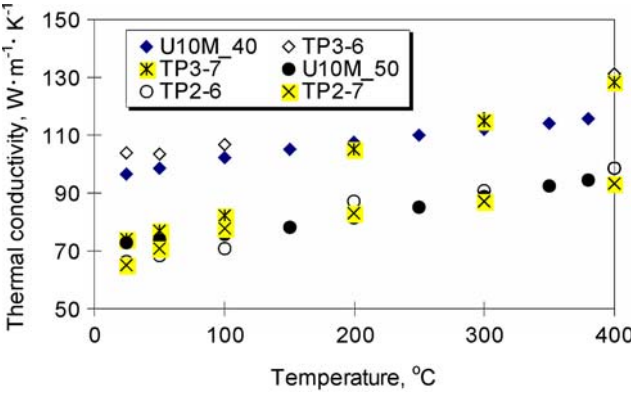

Fig. 8. Comparison between reference values with a similar uranium loading density, gU· cm^{-3} and thermal conductivity of U–8 mass% Mo/Al.

the uranium loading density increased with a significant difference observed at various temperatures. The density differences were controlled by the volume fraction of U–Mo. Furthermore, this had a significant impact on the thermal conductivity.

4. CONCLUSION

The thermal conductivities of dispersion fuels were determined from measurements of the thermal diffusivity, specific heat capacity, and den-

Table XIV. Comparison of the Thermal Conductivity of U–10 wt.% Mo/Al Dispersion Fuel

Sample T (°C)	U10M_A40 ($W \cdot m^{-1} \cdot K^{-1}$)	TP3-6 ($W \cdot m^{-1} \cdot K^{-1}$)	TP3-7 ($W \cdot m^{-1} \cdot K^{-1}$)	U10M_A50 ($W \cdot m^{-1} \cdot K^{-1}$)	TP2-6 ($W \cdot m^{-1} \cdot K^{-1}$)	TP2-7 ($W \cdot m^{-1} \cdot K^{-1}$)
25	96.5	103.9	74.0	73.0	66.5	65.1
50	98.6	103.6	77.0	73.7	68.2	70.7
100	102.2	106.8	82.1	75.7	70.9	77.8
150	105.2	–	–	78.3	–	–
200	107.7	105.1	105.1	81.4	87.1	83.1
250	109.9	–	–	84.9	–	–
300	112.0	115.9	114.7	88.6	90.9	87.3
350	114.1	–	–	92.4	–	–
380	115.5	–	–	94.6	–	–
400	–	131.4	128.2	–	98.5	93.2
500	–	124.9	124.8	–	100.1	93.3

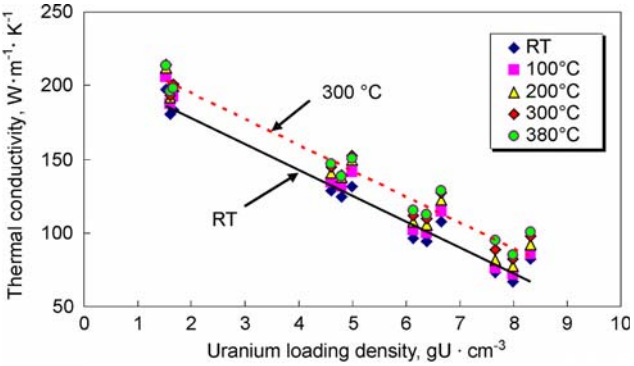

Fig. 9. Thermal conductivity of all samples per uranium loading density, gU· cm^{-3}.

sity. The thermal conductivity of dispersion fuels predominantly increased with temperature and decreased with an increase in the volume fraction of U–Mo. The thermal conductivity of the specimen fabricated with the centrifugal atomized method was found to be more reliable than that of the material fabricated with the comminution method. Excluding some data with a large discrepancy compared to the results of Taylor [12], the overall data matched other results for similar systems within about 5%. The fabrication of powders was quite different between Taylor and this study. The U–Mo powder made by the atomization method used here has a spherical

shape and uniform size distribution. But in the work of Taylor, his specimens were fabricated from U–Mo powder by the mechanical grinding method, resulting in irregular-shaped particles. Therefore, the fabrication method is thought to have a strong affect on the thermal conductivity. The effect of the fabrication method on the thermal conductivity in U_3Si/Al dispersion fuels was reported earlier [13]. The thermophysical property data from this current study can be useful in core temperature evaluation of nuclear fuel and in the thermal design in utilizing nuclear fuel in a nuclear reactor.

REFERENCES

1. S. H. Lee, J. C. Kim, J. M. Park, and C. K. Kim, *Int. J. Thermophys.* **24**:1355 (2003).
2. C. K. Kim, H. J. Ryu, J. M. Park, K. H. Kim, H. R. Kim, and K. H. Lee, *Proc. 2000 Int. Meeting on Reduced Enrichment for Research and Test Reactors*, ANL/TD/TM01-12 (2000), p. 233.
3. S. L. Hayes, C. R. Clark, J. R. Stuart, and M. K. Meyer, *Proc. 2000 Int. Meeting on Reduced Enrichment for Research and Test Reactors*, ANL/TD/TM01-12 (2000), p. 225.
4. K. H. Kim, D. B. Lee, C. K. Kim, and I. H. Kuk, *Proc. 19th Int. Meeting on Reduced Enrichment for Research and Test Reactors*, Seoul, Korea (1996).
5. G. L. Hofman, M. K. Meyer, and A. E. Ray, *Proc. 21st Int. Meeting on Reduced Enrichment for Research and Test Reactors*, Sao Paulo, Brazil (1998).
6. J. M. Park, Y. S. Han, K. H. Kim, Y. S. Lee, and C. K. Kim, *Proc. 22nd Int. Meeting on Reduced Enrichment for Research and Test Reactors*, Budapest, Hungary (1999).
7. K. H. Kim, H. J. Kwon, J. S. Lee, H. J. Ryu, J. M. Park, and C. K. Kim, *Proc. 2000 Int. Meeting on Reduced Enrichment for Research and Test Reactors*, ANL/TD/TM01-12 (2000), p. 285.
8. S. H. Lee, J. C. Kim, J. M. Park, H. J. Ryu, and C. K. Kim, *Proc. 2000 Int. Meeting on Reduced Enrichment for Research and Test Reactors*, ANL/TD/TM01-12 (2000), p. 261.
9. W. J. Parker, R. J. Jenkins, C. P. Butler, and G. L. Abbott, *J. Appl. Phys*. **32**:1679 (1961).
10. T. Azumi and Y. Takahashi, *Rev. Sci. Instrum*. **52**:1411 (1981).
11. J. Emsley, *The Elements*, 2nd Ed. (Oxford University Press, Oxford, 1990).
12. R. E. Taylor, *TPRL Report 2368* (2000), p. 4.
13. W.-S. Ryu, J.-M. Park, C.-K. Kim, and I.-H. Kuk, *Proc. 1994 Int. RERTR Meeting*, Williamsburg, Virginia (1994).